OPEN

NPG Asia Materials (2015) 7, e148; doi:10.1038/am.2014.114

www.nature.com/am

ORIGINAL ARTICLE

Bio-inspired controlled release through compression–relaxation cycles of microcapsules

Yue Long[1], Chuanyong Liu[2], Bin Zhao[2], Kai Song[1], Guoqiang Yang[2] and Chen-Ho Tung[2]

The aim of microencapsulation is to achieve controllable and sustainable release at the desired site. Despite the many methods developed in recent years, there is still a need to advance the strategies for higher controllability and scalability. Taking inspiration from the heart, which pumps blood by continual contraction of muscles, we demonstrate a novel releasing method, in which the core release is controlled by the compression–relaxation cycles of microcapsules upon the application of a magnetic field. This idea is realized by embedding Fe_3O_4 particles into a polymer shell. When the magnetic field is applied, the Fe_3O_4 particles align along the field direction and stretch the shell, resulting in compression of the microcapsules and release of the core contents; the shape is restored after the field is removed. We demonstrated various release patterns by altering the strength of the magnetic field and the compression frequency. This release method provides repeated and pulsatile delivery, enhanced spreading distance and ejection speed, and is site specific and proactive, providing a new option for controlled release applications.
NPG Asia Materials (2015) **7,** e148; doi:10.1038/am.2014.114; published online 9 January 2015

INTRODUCTION

In microencapsulation research, the optimum goal is to release the core contents at the appropriate time and place and in a controlled manner. Considerable effort has been devoted to achieving this goal via incorporation of functional materials or nanoparticles into the microcapsule shell to control the release of the contents of the microcapsules through the application of an external stimulus,[1–3] such as pH,[4–7] temperature,[8–10] light,[11–13] ultrasound,[14–17] glucose[18,19] and magnetic field,[20–22] at the appropriate time. Significant progress has been achieved to develop such controlled release methods; however, methods with better controllability are still in demand. Until now, two strategies have been used for initiating changes in a microcapsule shell, thereby controlling the release. The first strategy is diffusion based that focuses on switching or tuning the size of pores in the shell to influence the diffusion rate of the contents of the core; the second strategy is mainly based on the destruction of the shell, resulting in a near instantaneous core release, that is, a burst release. However, in certain application areas, a release system that has a relatively higher release velocity compared with passive diffusion and better controllability over the burst release is especially desired.[23]

Undoubtedly, the most direct way to release the core contents for a liquid-containing object with a permeable shell is to compress the container and force the core to flow through the holes. If the compression force is well controlled, then sustained release is achievable. In the blood circulation system, the heart pumps the blood out by continual contraction of muscles to maintain the blood flow. Similar phenomena can be widely found in organisms that inject liquids by contracting muscles and deforming part of the body or the entire body. Nevertheless, because of the microscaled size, the force required for compressing a single microcapsule is 0.1–100 μN.[24,25] Such small forces make it difficult to precisely control the deformation of the microcapsules without rupturing the shell. Recently, a technique utilizing an atomic force microscopy cantilever with a glass bead attached to its tip to compress an individual microcapsule to release the core contents was developed.[26–28] Being different from passive diffusion-based or burst release, this approach provides the possibility of accelerating the release of microcapsules in a controlled manner, while maintaining the integrity of the shell. Furthermore, pressurized release enabled larger spreading distances and anisotropic release.[28] Nevertheless, because of its cantilever-based operating system, this technique is only limited to the study of single microcapsules.

In this study, being inspired by the heart, composite microcapsules with Fe_3O_4 particles embedded in the elastic polymer shell were fabricated. Under the application of a magnetic field, microcapsules are compressed to release the core contents; when the field is removed, the shape is restored. Thus, this cycle could be performed consecutively to provide repeated and pulsatile delivery during the releasing process, similar to the manner that the heart contracts and pumps blood out. Thus, the release rate of the core contents can be well controlled by the frequency of the compression–relaxation cycles or/and the degree of deformation of the microcapsules.

[1]Laboratory of Bio-Inspired Smart Interface Science, Technical Institute of Physics and Chemistry, Chinese Academy of Sciences, Beijing, China and [2]Beijing National Laboratory for Molecular Sciences, Key Laboratory of Photochemistry, Institute of Chemistry, Chinese Academy of Sciences, Beijing, China
Correspondence: Professor K Song, Laboratory of Bio-Inspired Smart Interface Science, Technical Institute of Physics and Chemistry, Chinese Academy of Sciences, Beijing 100190, China.
E-mail: songkai@mail.ipc.ac.cn
Received 25 September 2014; revised 1 November 2014; accepted 4 November 2014

EXPERIMENTAL PROCEDURE

Chemicals

Ferric chloride ($FeCl_3$, anhydrous) and sodium acetate (anhydrous, NaAc) were purchased from Acros (Beijing, China). *N*-isopropylacrylamide (NIPAm), *N*, *N*'-methylenebisacrylamide (MBAm), fluorescein isothiocyanate (FITC)–dextran (molecular weight 40K) and 2,2'-azobis(2-methylpropionamidine)dihydrochloride (AIBA) were purchased from Sigma-Aldrich (Shanghai, China). Ethylene glycol, ethanol, oleic acid and hexane were purchased from Beijing Chemical Works (Beijing, China). Polyethylene glycol (molecular weight ~2000) was purchased from Alfa Aesar (Shanghai, China). All the chemicals were used as received. The water used throughout all the experiments was purified using the Millipore system (Beijing, China).

Preparation of Fe_3O_4 microparticles

In a typical synthesis of Fe_3O_4 microparticles, NaAc (2.7 g) was dissolved in ethylene glycol (20 ml), and the solution was kept in a water bath at 50 °C. $FeCl_3$ (0.811 g) was dissolved in ethylene glycol (10 ml) to form a clear solution, followed by the addition of polyethylene glycol (0.75 g), and water (0.54 ml) was added into the resulting solution after polyethylene glycol was dissolved completely. Next, the mixture was poured into the NaAc solution slowly while stirring vigorously in the water bath at 50 °C, and the stirring was maintained for 2 h. The resulting brownish-yellow solution was sealed in a Teflon-lined stainless-steel autoclave and then kept at 200 °C for 4 h in the oven. After being cooled to room temperature, the dark products were collected by a magnet and washed with ethanol and water (1:1) several times until the supernatant was clear. The products were then transferred to pure ethanol (30 ml). To the resulting dispersion, oleic acid (1 ml) was added to render hydrophobicity to the particles. Next, the mixture was sonicated for 30 min before being placed in the Teflon-lined autoclave and heated in the oven at 70 °C. After 2 h, the products were cooled to room temperature and then washed with ethanol and water (1:1) before drying in air.

Preparation of the microcapsules

Fe_3O_4 microparticles (0.05 g) were dispersed in hexane (6 ml) and sonicated for 10 min at room temperature. An aqueous solution (0.9 ml) of NIPAm (33 mg), MBAm (3.3 mg) and AIBA (1.67 mg) was poured into the Fe_3O_4 dispersion, followed by emulsifying for 2 min by manual shaking. The resulting water-in-oil (w/o) emulsion was deoxygenated by bubbling through nitrogen gas for 20 min at room temperature before increasing the temperature to 60 °C; the temperature was maintained for 6 h. The dark dispersions were then cooled to room temperature and washed with ethanol 3 times. Finally, the resulting products were transferred into water.

Controlled release of the microcapsules

The microcapsules were transferred into an aqueous FITC–dextran solution and kept in the dark. After 12 h, the microcapsules were washed several times with pure water until the fluorescence intensity of the supernatant was nearly zero. In a release test without applying a magnetic field, an aqueous dispersion of microcapsules (3 ml) was placed in the dark; the sample was shaken to ensure that the dispersion was well mixed, and then an aliquot (0.2 ml) was taken from the supernatant solution at various time intervals between 1 and 60 min after the microcapsules sunk to the bottom of the container, which only took a few seconds. The fluorescence intensity of the solution was examined using a fluorometer. The release of the microcapsules with an external magnetic field was performed the same way, with the only exception being that a permanent magnet was held under the sample vial for 2 min and then removed for ~30 s before subjecting the sample to the magnetic field again. This cycle was repeated during the measurement. For the multi-stage release experiment, for each compression cycle, the magnetic field was applied for 30 s and then relaxed for another 30 s in the magnetic field ON state.

Characterization

X-ray diffraction analysis was performed with a D/Max 2500V/PC X-ray diffractometer in the 2θ range of 10–70° using Cu-K_α radiation ($\lambda = 1.54056$ Å). Scanning electron microscope images were obtained using a JEOL S-4800 field emission scanning electron microscope (Tokyo, Japan). Transmission electron microscope (TEM) images and high-resolution TEM images were taken using a JEOL JEM-2100F TEM. The magnetic properties were investigated using a SQUID vibration sample magnetometer (Lake Shore Cryotronics, Westerville, OH, USA). The fluorescence intensity was examined using a fluorometer (Hitachi, F-2500, Tokyo, Japan). The fluorescence of the microcapsules was visualized using a fluorescent microscope (Olympus, BX53, Tokyo, Japan).

RESULTS

Preparation of the magnetic microcapsules

In this study, the microcapsules of sub-millimeter size were fabricated to facilitate the optical observation of the magnetic field-induced deformation and release, whereas nano-scaled microcapsules are more suited for *in vivo* delivery and will be investigated in subsequent studies. The Fe_3O_4 particles used to form the Pickering emulsion were prepared using a solvothermal method. The average diameter of the produced particles is ~600 nm, and the particles exhibited a magnetic saturation of 82.4 emu g^{-1} (details regarding the characterization of the Fe_3O_4 particles are available in the Supplementary Information S1, including scanning electron microscope and TEM images, X-ray diffraction patterns and magnetization curve of the Fe_3O_4 particles).

Composite microcapsules were prepared by utilizing Pickering emulsion as a template to embed colloidal particles in the shell. A microcapsule prepared in such a manner is also called a 'colloidosome'.[29] Here, as shown in Figure 1, an aqueous solution of NIPAm monomer, initiator and crosslinker was first mixed with a hexane dispersion of hydrophobic Fe_3O_4 particles. After vigorous shaking, a w/o emulsion was formed with the Fe_3O_4 particles located at the w/o

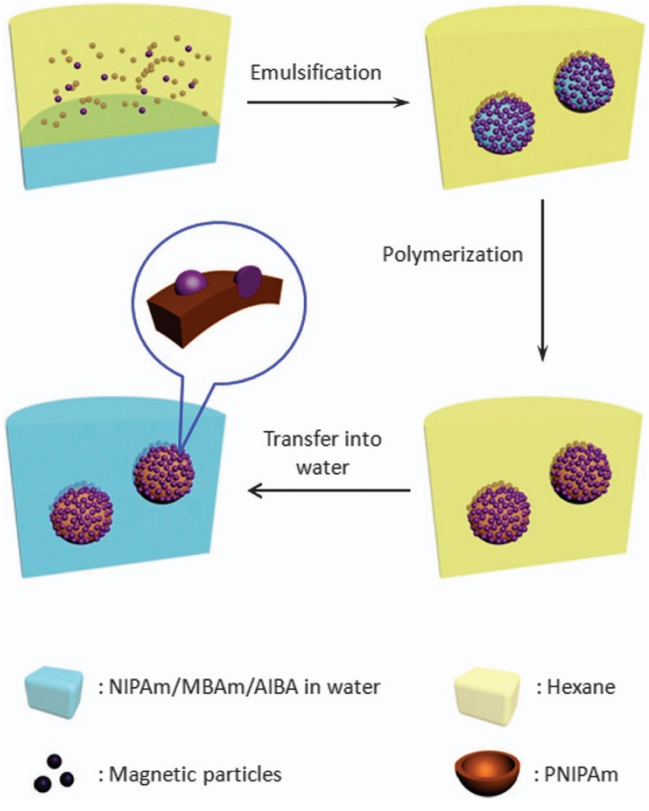

Figure 1 Schematic representation of the preparation of the composite microcapsules. The inset is an enlarged illustration of the partial entrapment of Fe_3O_4 microparticles in the poly(*N*-isopropylacrylamide) (PNIPAm) shell. AIBA, 2,2'-azobis(2-methylpropionamidine)dihydrochloride; MBAm, *N*,*N*'-methylenebisacrylamide; NIPAm, *N*-isopropylacrylamide.

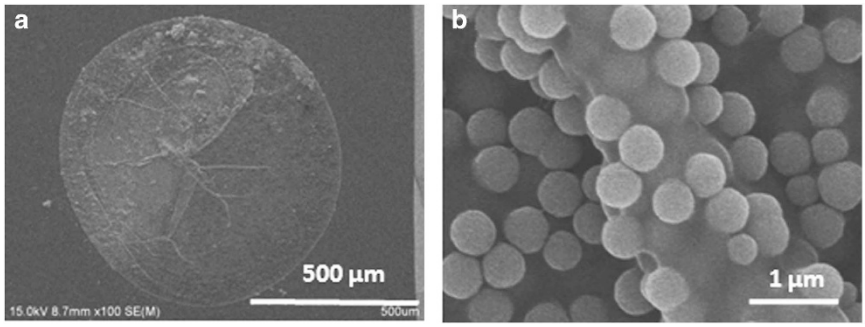

Figure 2 (**a**) Overview scanning electron microscope (SEM) image of the composite microcapsule with magnetic particles embedded in the shell. (**b**) Magnified SEM image of the microcapsule shell.

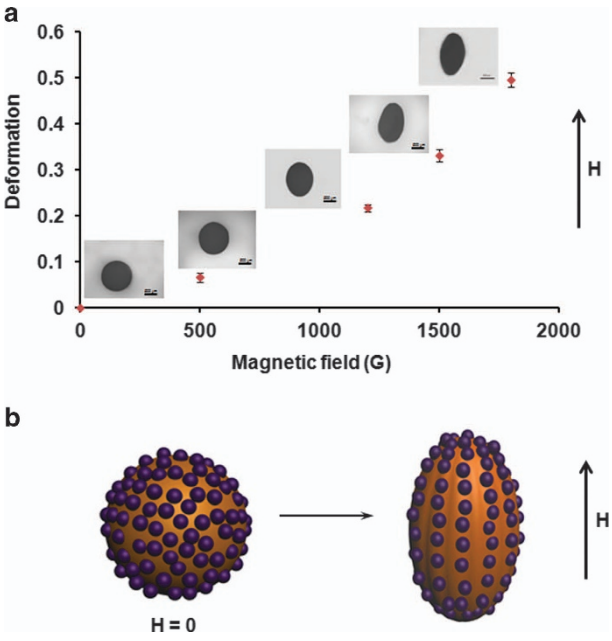

Figure 3 Deformation of microcapsules under an external static magnetic field. (**a**) Deformation of microcapsules as a function of a magnetic field (30 microcapsules were measured for each sample). The insets are optical microscopic images of the microcapsules under different magnetic field strengths. (**b**) Schematic representation of the deformation mechanism of microcapsules under the magnetic field. All the scale bars in the inset images are 500 μm.

interface. Upon increasing the temperature, NIPAm monomers in the water droplet started to polymerize. As a well-known thermosensitive polymer, poly(*N*-isopropylacrylamide) (PNIPAm) exhibits a hydrophilic–-hydrophobic transition at its lower critical solution temperature of 32 °C. Hence, at elevated temperatures, the polymerized hydrophobic PNIPAm would migrate and deposit onto the oil/water interface, locking the Fe_3O_4 particles within the polymer network to produce the composite microcapsule shell.

Morphology of microcapsules

An optical microscopic image of microcapsules dispersed in water (available in Supplementary Figure S2) reveals that they are spherically shaped and can be transferred into the aqueous phase without any deformation or rupturing. In addition, the scanning electron microscope image shown in Figure 2a indicates that the shell is completely overlapped after losing its core contents in the sampling process. This result is because of the soft and thin polymer membrane that cannot hold its original shape after losing the core contents; the image also proves the hollow structure of microcapsules. A closer inspection of the microcapsule shell in Figure 2b reveals that the Fe_3O_4 particles are densely packed with some particles embedded, and the other particles are attached to the surface of the polymer membrane. From the folded part, the thickness of the shell can be roughly calculated. As the width of the folding shell is ~2 μm, the average diameter of the Fe_3O_4 nanoparticles is ~600 nm, and the thickness of the polymer is only a few hundred nanometers or even less. This delicate thin shell enables the microcapsule to exhibit flexibility and softness, essential for deformation of the shell.

Deformation of microcapsules under a static magnetic field

Deformation ($D = (a - b)/R$, where a and b are the semi-major and semi-minor axes of the resulted ellipsoid, respectively, and R is the radius of the original sphere) of the microcapsules as a function of the magnetic field is plotted and shown in Figure 3a. As demonstrated by the insets, the spherical microcapsules elongated along the magnetic field direction when applying a static magnetic field. The microcapsules deformed further as the strength of the magnetic field increased, until reaching its maximum deformability at 1800 G. A further increase in the magnetic field above 1800 G was observed to not further deform the microcapsule. Neglecting the expansion of the surface area of the shell, any deformation of the microcapsule from the spherical shape will decrease the volume and consequently increase the inner osmotic pressure. At 1800 G, the deformation is ~0.5. Assuming the deformed shape is a standard ellipsoid, the volume at this stage is ~72% of the initial shape. Upon removal of the field, the microcapsules returned to their initial shape within a few seconds. Such a rapid restoration of shape endows the possibility of circulatory compression to the microcapsules during the release. The plot from Figure 3a also reveals that the deformation is proportional to H^2, in agreement with the previous theoretical study.[30] The deformation of the microcapsules with different wall thicknesses was also monitored (experimental details are shown in Supplementary Information S3, and videos of the deformation of different microcapsules are available in Supplementary Movies S1–S3. The direction of the applied magnetic field in the movie is orthogonal to the focal plane; hence, deformation of microcapsules manifests as shrinkage). The results indicate that microcapsules fabricated by the current method displayed the optimum deformability without destroying the shell. Microcapsules with a thicker wall exhibited smaller deformation, and those with a thinner wall were easily damaged during the washing and deformation processes.

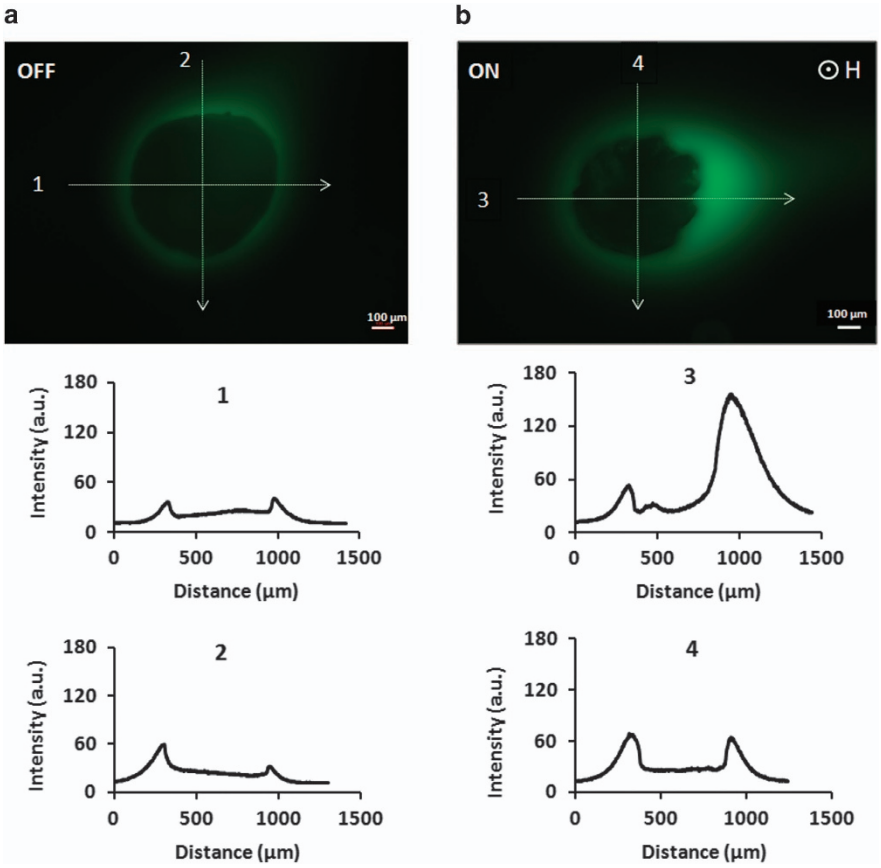

Figure 4 Fluorescent microscopic images of the release of fluorescein isothiocyanate (FITC)–dextran from the microcapsules. (**a**) A single microcapsule before application of a magnetic field; curves 1 and 2 are the fluorescence intensity distributions of the areas covered by lines 1 and 2, respectively. (**b**) After applying a magnetic field of 1800 G, curves 3 and 4 are the fluorescence intensity distributions of the areas covered by lines 3 and 4. All the scale bars are 100 μm.

The mechanism of microcapsule deformation is presented in Figure 3b. The driving force of this deformation is believed to be because of the induced magnetic dipole moment formed when a paramagnetic particle is placed in an external magnetic field that orients the particle parallel to the direction of the magnetic field. When the external magnetic field was of sufficient strength, the magnetic moment of the particle reached a saturated value. This induced dipole moment resulted in an attractive dipole–dipole force along the field direction that drove the particles to form a one-dimensional chain-like structure along the dipole moments. When the magnetic particles were enwrapped in the polymer, this alignment of the particles caused the elongation of the microcapsule along the field direction, resulting in contraction in the perpendicular direction to maintain the same surface area. Upon removal of the field, the magnetic dipole moment quickly randomized, and the magnetization reduced to zero; as a result, the arrangement of the Fe_3O_4 particles in the polymer shell recovered and allowed the fluid from the outer bulk phase to flow back into the microcapsule through the pores in the shell, thereby enabling the microcapsule to return to its initial shape.

Release

A dye, FITC–dextran, was used as a model drug to monitor the release of magnetically controlled microcapsules. Fluorescent microscopic images of the microcapsules were obtained, as shown in Figure 4, to visually monitor the deformation-induced release. Because of the close packing of the Fe_3O_4 nanoparticles in the membrane, both the incident and fluorescent light of the core are shielded; as a result, only released fluorescent core material can be seen from the image. As shown in the images, two directional lines (indicated by the arrows) are drawn across the microcapsule, and the fluorescence intensities along each line were measured and plotted below each image. The two peaks of the curves correspond to the strongest fluorescence intensities at the edges of the microcapsule. Before application of the magnetic field, slow release of the fluorescent core contents was observed, with the highest intensity of 40–60 (Figure 4a). From the figure, the two distribution curves in both directions (lines 1 and 2) are very similar, indicating the uniform release around the microcapsule shell. In contrast, when the magnetic field was applied (Figure 4b), the microcapsule started to deform. The direction of the applied field in this image was orthogonal to the focal plane to facilitate the observation of the release; as a result, the deformation was manifested as shrinkage of the microcapsule rather than elongation. The image in Figure 4b was obtained as the deformation reached the maximum, occurring a few seconds after being subjected to the magnetic field (a video of the deformation release of the microcapsule is available in Supplementary Movie S4).

In addition, as evidenced by the fluorescent image, upon deformation, more of the encapsulated fluorescent dye extruded out of the microcapsule in an anisotropic manner, with the right side appearing brighter than the other parts. This release pattern is also confirmed by

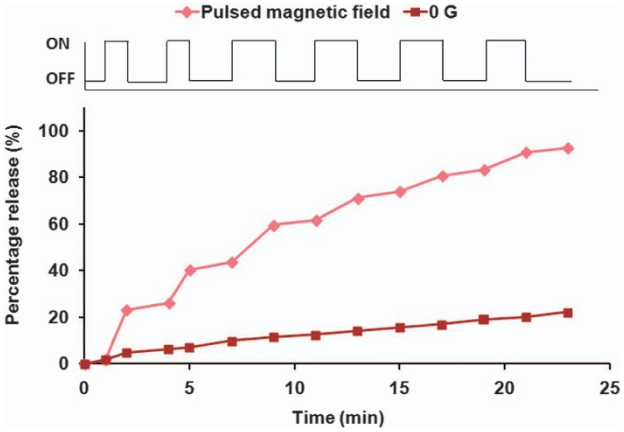

Figure 5 Release curve of microcapsules under a pulsed magnetic field at 1800 G with 2 min intervals between each application, as shown by the ON/OFF bar on the top, compared with the release curve of microcapsules without a magnetic field applied.

the intensity curve presented below the image (lines 3 and 4). The fluorescence intensities of the peaks were found to be all higher than those without the magnetic field in both directions. The highest fluorescence intensity that appeared on line 3 is 156, which is ~3 times the intensity value in the same position of line 1. In addition, the span of this peak is ~6 times larger than the peak without the magnetic field.

The larger spreading area of the core contents is a direct indication of the higher internal osmotic pressure and higher flow rate because of deformation. In accord with the visual observation, both the intensity and the span of the peak of line 3 are considerably larger than the other peaks, supporting the fact that the core contents were released from the deformed microcapsule in an anisotropic manner. This anisotropic phenomenon was observed in most of the microcapsules, and this can be attributed to the nonuniform thickness of the membrane shell during the formation process. This anisotropic release was not observed in the diffusion-based release (Figure 4a), whereas it was enhanced under the effect of the magnetic field; this anisotropic release might be useful for directional release in potential applications. Note that wrinkles appeared on the surface of the microcapsule shell during the deformation, a strong indication of the volume reduction of the microcapsule.

To further quantify the effect of the magnetic field on the release of the microcapsules, the sample was subjected to a magnetic field of 1800 G with a 2-min interval between each application. The release was studied via time-resolved measurement of the fluorescence intensity of the outer bulk solution over 23 min using a fluorometer (Figure 5). The percentage release of core contents is calculated by Equation (1):

$$M = \frac{M_t}{M_0} \times 100\% \quad (1)$$

where M_t is the amount of FITC–dextran released at time t and M_o is the total encapsulated FITC–dextran in the microcapsules (M_o is evaluated by breaking the microcapsules via ultrasonication and then measuring the fluorescence intensity of the supernatant solution).

The curves in Figure 5 reveal that core release exhibits sharp amplifications in response to each magnetic field application. This sudden increase in the release rate is believed to be induced by deformation, which agrees with the observation described above. In comparison with the release curve without the stimulation of a

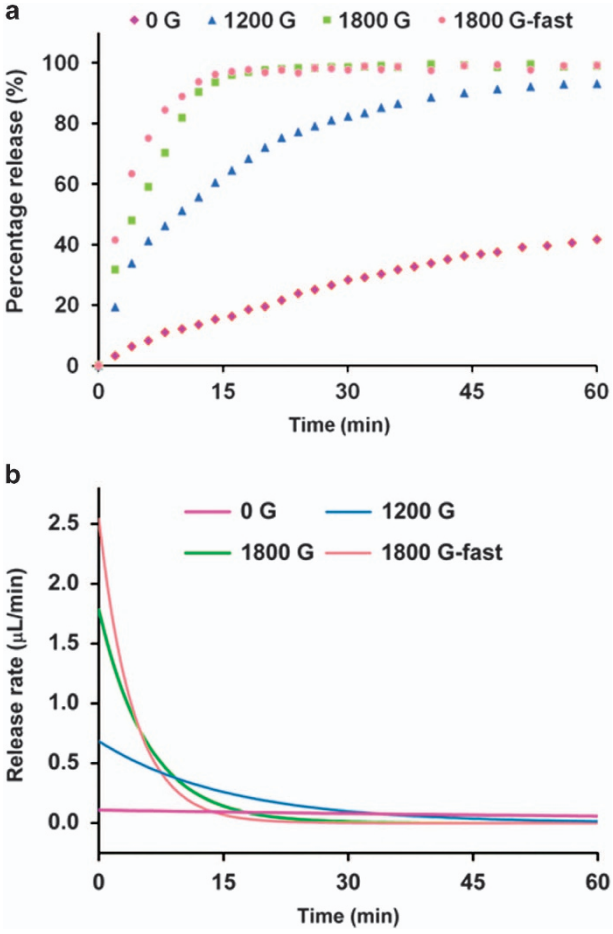

Figure 6 Release profile of the microcapsules. (**a**) Accumulated release of microcapsules under magnetic field strengths of 0, 1200, 1800 and 1800 G with fast compression. (**b**) Release rate calculated from the release curves of (**a**). The graphs indicate that both a higher magnetic field and faster compression speed lead to more rapid release.

magnetic field, the core release reached ~92% in 23 min, whereas only ~24% of the core was released from the control sample (0 G). This multi-stage release is believed to be highly valuable in certain application areas, such as drug delivery. The ability to deliver therapeutic agents to a patient in a multi-staged release profile is considered to be more advantageous compared with the immediate burst release or the diffusion-based release. Multi-staged release offers better patient compliance, longer treatment duration and reduced side effects, thereby optimizing the therapeutic efficacy of drugs.

The release of microcapsules under different magnetic fields and different compression frequencies was also investigated. First, static magnetic fields of 0, 1200 and 1800 G were applied separately, and the accumulative release curves were recorded, as shown in Figure 6a. For each sample, 25 dye-containing microcapsules were randomly collected for the fluorescence measurement. During the 60 min release process, the accumulated release of core contents reached 42% at 0 G. However, it only took 6 min to achieve 42% release under a magnetic field of 1200 G and <4 min when an 1800 G magnetic field was applied. When the concentration of the inner core and the outside bulk solvent becomes similar, the release slows down and eventually stops. The curves of 1800 and 1200 G indicate that the release reached a plateau at ~24 min (98% release) and ~44 min (90% release), respectively. In comparison, at 0 G, the intensity of the outer bulk

phase increased continuously during 60 min, indicating that the release had not yet reached its equilibrium.

To further study the effect of compression frequency on the release rate, microcapsules were more frequently compressed and relaxed at 1800 G, with each of the cycle taking ~10 s (5 s of compression and 5 s of relaxation, denoted as 1800 G-fast), and the release curve is shown in Figure 6a. The faster compression was found to lead to a quicker release and a shorter time period to reach the equilibrium. This result was expected because more frequent compression promotes a more rapid exchange between the inner and outer fluids, accelerating the rate of release.

The various release kinetics of the microcapsules shown in Figure 6a were determined with the aim of quantifying the release of microcapsules under various magnetic stimuli. As shown in Figure 6a, the concentration of FITC–dextran in the outer bulk solution increased exponentially with time. Assuming that the volume released and refilled for each compression–relaxation process is the same, the exchange rate law can be presented as:[28]

$$\Delta V(t) = V_o - V_o \exp\left(\frac{-t}{\tau}\right) \quad (2)$$

where ΔV is the exchanged volume in each cycle, V_o is the total volume and τ is the time constant. After taking the time derivative of Equation (2), the volume flow rate Q can be expressed by:

$$Q(t) = \frac{V_o}{\tau} \times \exp\left(\frac{-t}{\tau}\right) \quad (3)$$

The plots of Equation (3) for microcapsules under different applied magnetic fields are presented in Figure 6b (calculations are available in Supplementary Information S4). From the equation, the initial flow rate of 25 microcapsules was obtained (the total volume of the microcapsules was calculated by multiplying the average volume of the microcapsules by the number of microcapsules, whereas the average volume of the microcapsules was obtained from measurements of 100 microcapsules): 0.11, 0.68, 1.78 and 2.54 μl min^{-1} for microcapsules at 0, 1200, 1800 and 1800 G-fast, respectively (calculations are shown in Supplementary Information S4). It can be seen that the initial flow rate increased by 6-, 16-, and 23-fold because of the effect of the magnetic fields of 1200, 1800, and 1800 G-fast, respectively. This result suggests that the velocity of release was significantly affected and controlled by the magnetic field; small changes in the field strength can result in large impacts on the release rate. After 60 min of the compression–relaxation process, all the microcapsules were found to retain their spherical shapes; this result demonstrates the good mechanical stability of the shell and is essential for future applications.

CONCLUSIONS

Microcapsules with Fe_3O_4 microparticles embedded in the PNIPAm polymer shell were fabricated based on the Pickering emulsion method. Upon application of the magnetic field, accelerated discharge of the core contents and enlarged spreading area were observed. The results also revealed that an increase in the magnetic field strength and/or compression frequency enables the increase in the release velocity. Compression–relaxation cycles could be consecutively performed during the release, acting as a magnetic pump, and the microcapsules can also be recycled by a magnetic field after the treatment. Therefore, for the first time, to our knowledge, we report the release of microcapsules controlled by compression–relaxation cycles through a magnetic field that mimics the muscle contraction of the heart. In comparison with the previous release approaches, this method endows sustained and pulsatile delivery and enhanced controllability over the release speed and is both safe and localizable. The results of this work will open a new path in utilizing magnetically responsive microcapsules in controlled delivery applications.

CONFLICT OF INTEREST

The authors declare no conflict of interest.

ACKNOWLEDGEMENTS

We acknowledge the State Basic Research Program of China (2013CB834505) and the program of the National Natural Science Foundation of China (21273248) for their financial support. Yue Long acknowledges the Chinese Postdoctoral Science Foundation Grant (2012M520390).

1 Wohl, B. M. & Egbersen, F. J. Responsive layer-by-layer materials for drug delivery. *J. Control. Release* **158**, 2–14 (2012).
2 Delcea, M., Möhwald, H. & Skirtach, A. G. Stimuli-responsive LbL capsules and nanoshells for drug delivery. *Adv. Drug Deliver. Rev.* **63**, 730–747 (2011).
3 Esser-Kahn, A. P., Odom, S. A., Sottos, N. R., White, S. R. & Moore, J. S. Triggered release from polymer capsules. *Macromoleucles* **44**, 5539–5553 (2011).
4 Wang, A., Cui, Y., Li, J. B. & van Hest, C. M. Fabrication of gelatin microgels by a 'cast' strategy for controlled drug release. *Adv. Funct. Mater.* **22**, 2673–2681 (2012).
5 Diéguez, L., Darwish, N., Graf, N., Vörös, J. & Zambelli, T. Electrochemical tuning of the stability of PLL/DNA multilayers. *Soft Matter* **5**, 2415–2421 (2009).
6 Miguel, A. S. & Behrens, S. H. Permeability control in stimulus-responsive colloidosomes.. *Soft Matter* **7**, 1948–1956 (2011).
7 Kozlovskaya, V., Wang, Y., Higgins, W., Chen, J., Chen, Y. & Kharlampieva, E. pH-triggered shape response of cubical ultrathin hydrogel capsules. *Soft Matter* **8**, 9828–9839 (2012).
8 Basset, C., Harder, C., Vidaud, C. & Déjugnat, C. Design of double stimuli-responsive polyelectrolyte microcontainers for protein soft encapsulation. *Biomacromolecules* **11**, 806–814 (2010).
9 Cao, Z. H., Landfester, K. & Ziener, U. Preparation of dually, pH- and thermo-responsive nanocapsules in inverse miniemulsion. *Langmuir* **28**, 1163–1168 (2012).
10 Chandrawati, R., Odermatt, P. D., Chong, S. F., Price, A. D., Städler, B. & Caruso, F. Triggered cargo release by encapsulated enzymatic catalyst in capsosomes. *Nano Lett.* **11**, 4958–4963 (2011).
11 Volodkin, D. V., Madaboosi, N., Blacklock, J., Skirtach, A. G. & Möhwald, H. Surface-supported multilayers decorated with bio-active material aimed at light-triggered drug delivery. *Langmuir* **25**, 14037–14043 (2009).
12 Kurapati, R. & Raichur, A. M. Near-infrared light-responsive graphene oxide composite multilayer capsules: a novel route for remote controlled drug delivery. *Chem. Commun.* **49**, 734–736 (2013).
13 Xu, W., Choi, I., Plamper, F. A., Synatschke, C. V., Müller, A. H.E. & Tsukruk, V. V. Nondestructive light-initiated tuning of layer-by-layer microcapsule permeability. *ACS Nano* **7**, 598–613 (2013).
14 Lensen, D., Gelderblom, E. C., Vriezema, D. M., Marmottant, P., Verdonschot, N., Versluis, M., de Jong, N. & van Hest, J. C.M. Biodegradable polymeric microcapsules for selective ultrasound-triggered drug release. *Soft Matter* **7**, 5417–5422 (2011).
15 Skirtach, A. G., De Geest, B. G., Mamedov, A., Antipov, A. A., Kotov, N. & Sukhorukov, G. B. Ultrasound stimulated release and catalysis using polyelectrolyte multilayer capsules. *J. Matter. Chem.* **17**, 1050–1054 (2007).
16 De Geest, B. G., Skirtach, A. G., Mamedov, A. A., Antipov, A. A., Kotov, N. A., De Smedt, S. C. & Sukhorukov, G. B. Ultrasound-triggered release from multilayered capsules. *Small* **3**, 804–808 (2007).
17 Jing, Y. J., Zhu, Y., Yang, X., Shen, J. & Li, C. Ultrasound-triggered smart drug release from multifunctional core-shell capsules one-step fabricated by coaxial electrospray method. *Langmuir* **27**, 1175–1180 (2011).
18 Qi, W., Duan, L., Wang, K. W., Yan, X. H., He, Q. & Li, J. B. Motor protein CF0F1 reconstituted in lipid-coated hemoglobin microcapsules for ATP synthesis. *Adv. Mater.* **20**, 601–605 (2008).
19 Qi, W., Yan, X., Duan, L., Cui, Y., Yang, Y. & Li, J. Glucose-sensitive microcapsules from glutaraldehyde cross-linked hemoglobin and glucose oxidase. *Biomacromoleucules* **10**, 1212–1216 (2009).
20 Katagiri, K., Imai, Y., Koumoto, K., Kaiden, T., Kono, K. & Aoshima, S. Magnetoresponsive on-demand release of hybrid liposomes formed from Fe3O4 nanoparticles and thermosensitive block copolymers. *Small* **7**, 1683–1689 (2011).
21 Sukhorukov, G., Rogach, A. L., Garstka, M., Springer, S., Parak, W. J., Muñoz-Javier, A., Kreft, O., Skirtach, A. G., Susha, A. S., Ramaue, Y., Palankar, R. & Winterhalter, M. Multifunctionalized polymer microcapsules: novel tools for biology and pharmacological applications. *Small* **3**, 944–955 (2007).
22 Hu, S. H., Tsai, C. H., Liao, C. F., Liu, D. M. & Chen, S. Y. Controlled rupture of magnetic polymelectrolyte microcapsules for drug delivery. *Langmuir* **24**, 11811–11818 (2008).

23 Bruns, P. J. & Cassidy-Hanley, D. *Methods in Cell Biology* Vol. 62, 501 (Academic Press, San Diego, CA, USA, 2000).
24 Gordon, V. D., Chen, X., Hutchinson, J. W., Bausch, A. R., Marquez, M. & Weitz, D. A. Self-assembled polymer membrane capsules inflated by osmotic pressure. *J. Am. Chem. Soc.* **126**, 14117–14122 (2004).
25 Wang, Q. G., Nguyen, B., Thomas, C. R., Zhang, Z., Alicia, J., Haj, E. I. & Kuiper, N. J. Molecular profiling of single cells in response to mechanical force: comparison of chondrocytes, chondrons and encapsulated chondrocytes. *Biomaterials* **31**, 1619–1625 (2010).
26 Delcea, M., Schmidt, S., Palankar, R., Fernandes, P. A.L., Fery, A., Möhwald, H. & Skirtach, A. G. Mechanobiology: correlation between mechanical stability of microcapsules studied by AFM and impact of cell-induced stresses. *Small* **6**, 2858–2862 (2010).
27 Fernandes, P. A.L., Delcea, M., Skirtach, A. G., Möhwald, H. & Fery, A. Quantification of release from microcapsules upon mechanical deformation with AFM. *Soft Matter* **6**, 1879–1883 (2010).
28 Schmidt, S., Fernandes, P. A.L., De Geest, B. G., Delcea, M., Skirtach, A. G., Möhwald, H. & Fery, A. Release properties of pressurized microgel templated capsules. *Adv. Funct. Mater.* **21**, 1411–1418 (2011).
29 Dinsmore, A. D., Hsu, M. F., Nikolaides, M. G., Marquez, M., Bausch, A. R. & Weitz, D. A. Colloidosomes: selectively permeable capsules composed of colloidal particles. *Science* **298**, 1006–1009 (2002).
30 Raikher, Y. L. & Stolbov, O. V. Magnetodeformation effect in a ferroelastic material. *Tech. Phys. Lett.* **26**, 156–158 (2000).

Supplementary Information accompanies the paper on the NPG Asia Materials website (http://www.nature.com/am)